

RE-ORDER NO. 64-661

N65-20620

25
CR-57591
PLANS ON THIS OR AS REFERRED

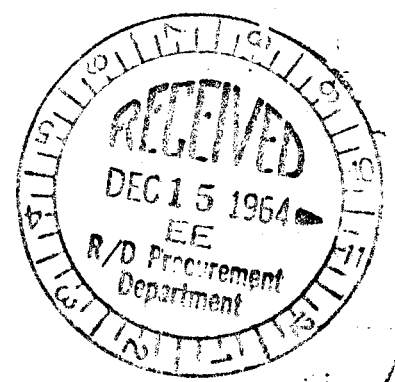
1
39
DATE

**EFFECT OF IMPACT VELOCITY ON THE PERFORMANCE
OF SEVERAL ENERGY ABSORPTION MATERIALS**

BY

Anthony P. Coppa
Research Engineer
Space Sciences Laboratory

This work was performed for the Jet Propulsion Laboratory,
California Institute of Technology, sponsored by the
National Aeronautics and Space Administration under
Contract NAS7-100.



This document submitted by the General Electric Company
Missile and Space Division in fulfillment of Jet Propulsion
Laboratory Purchase order nos: AR-4-331721, AR-4-331722.

GPO PRICE \$ _____
OTS PRICE(S) \$ _____

Hard copy (HCL) 8/1/65
Microfilm (MCL) 8/1/65

4/17/65

Series 3: Balsa Wood (parallel to grains)

Density	7.6 lb/ft ³ (typical)
Peak crushing stress	1500 psi (typical)

C. Description of the Tests

The tests were performed in the "Old Ironsides" impact facility located at the General Electric Company Missile and Space Division. In each test, the specimen, mounted on a relatively massive fixture, which was free to move along the line of impact, was impacted by the projectile. An accelerometer, attached at the rear surface of the mounting fixture, sensed the force transmitted to the mount via the specimen during the impact. Pertinent information applying to the tests are presented in Table I.

Deceleration was obtained directly from a Statham A5-500-350 strain gage type accelerometer for all tests except test no. 22 which employed an Endevco Type 2225 piezoelectric accelerometer whose output was run through a low pass Glennite filter.

D. Results

The results are presented in figures 1-25 and summarized in Tables 2-4. In figures 1-15, actual accelerometer records are presented together with pictures of the specimens after impact. Plots of the ratio of compressive stress/density versus unit axial shortening reduced from the accelerometer records are shown in figures 16-23 inclusive. The region of axial shortening covered in the plots is within the effective test interval and in most cases represents only the initial portion of the accelerometer records.

The specific energies were calculated from the formula:

$$K = \left(\frac{\sigma}{\rho} \right)_{\text{ave.}} \rho$$

where ρ is the thickness efficiency. Values of ρ used were as follows:

Material	ρ
Plastic honeycomb	.9
Aluminum honeycomb	.8 (obtained from these tests)
Balsa wood	.3

Values of specific energies are shown plotted against their corresponding impact velocities in Figures 24 and 25 for the nylon-phenolic and aluminum honeycombs respectively. Two curves of specific energy are shown for each material, K_1 and K_2 . K_1 is taken from the average stress which the material exhibits before the projectile impacts on the buffer ring in the impact apparatus. The interval between initial impact of the projectile in the specimen and the subsequent impact against the buffer ring is called the test interval since during it, the motion of the projectile is resisted only by the specimen and its axially unrestrained mount. Upon examination of the accelerometer records, it became evident that beyond the region of initial transient response of the specimen a region of rather constant stress usually was present. This constant level was considered to be more significant to an evaluation of the specific energy than the initial response, which in many cases comprised a significant part of the test interval. The value K_1 represents a specific energy which includes the initial response of the material. K_2 on the other hand, represents the specific energy of the material when it has reached quasi-steady state crushing and probably is

more indicative of a design value. Referring to Figure 24, both K_1 and K_2 decrease with velocity after peaking at the velocity of 166 ft./sec. The reason for the peaking is presently unexplained. The general decay of K_1 and K_2 with velocity is possibly linked to the effect of entrapped air in the cells, although the restriction of about 30% unit axial shortening in the test interval does not support this. Strain rate effect may be partially responsible. In any event, it does appear that the performance of at least this type of fiberglass honeycomb is deleteriously affected by higher impact velocities. It is to be noted that a value of specific energy of 22,500 ft. was obtained when material from the same log as that tested in the gun was impacted in the drop tester at a velocity of 25 ft./sec. In addition, the high specific energy of the material is indicated by its static compression stress value of 1360 psi minimum.

Turning now to Figure 25, it is evident that the specific energy of the aluminum honeycomb definitely increases with impact velocity. The curve for K_2 , which refers to the sustained value of stress, sweeps decidedly upward beyond a velocity of 250 ft./sec. and at $V_0 = 476$ ft./sec. K_2 is 18% higher than at $V_0 = 102$ ft./sec. Both K_1 and K_2 curves tend very well toward the static sustained crushing value of 11090 lb. ft./lb. as obtained from the supplier.

As contrasted with the plastic honeycomb, the behavior of the aluminum specimens was extremely orderly and free of breakup. Only the specimen of test No. 13 (Figure 9) exhibited a pond failure, and this was not a major one. On the other hand, improving the bond strength of the plastic honeycomb material will undoubtedly greatly improve its performance, since the breakup

Venting requirements should be analyzed and verified by experiment.

4. The effect of oblique impact on the performance of honeycombs under impact at high velocity should be evaluated experimentally.

5. The effect of higher impact velocity on the energy absorption performance of other useful materials than honeycombs should be evaluated.

Acknowledgement

The author gratefully acknowledges the dedicated efforts of Mr. Gregory P. Kernicky, Technician, Space Mechanics Operation, Space Sciences Laboratory, who performed the experiments.

Test No.	W_p grams	W_m grams	V_o ft/sec	$(\sigma/\rho)_1$ in $\times 10^4$	$(\sigma/\rho)_1$ ave. in $\times 10^4$	$(\sigma/\rho)_2$ in $\times 10^4$	$(\sigma/\rho)_2$ ave. in $\times 10^4$	K_1 ft	K_2 ft
1	7640	18,253	164	13.31	12.75	17.56	16.86	9560	12,640
2	7613		169	12.19		16.15			
3	7563		125	11.32	12.64	13.81	15.03	9430	11,470
4	7539		111	13.96		16.25			
6	7502		252	12.38	12.38	14.85	14.85	9235	11,140
7	7531		484	10.49	10.86	14.21	13.69	8145	10,270
13	7580		475	11.22		13.16			

Table 2. Impact Test Results on Nylon-Phenolic Fiberglass Honeycomb Material

The following list of symbols applies to all tables.

W_p , projectile weight; W_m , mounting fixture weight; $(\sigma/\rho)_1$, stress/density in the test interval;
 $(\sigma/\rho)_2$, stress/density representing a sustained constant level over a significant portion of the stroke;
 K_1 , specific energy corresponding to $(\sigma/\rho)_1$ ave.; K_2 , specific energy corresponding to $(\sigma/\rho)_2$ ave.

Test No.	W_p grams	W_m grams	V_o ft/sec	$(\sigma/p)_1$ in $\times 10^4$	$(\sigma/p)_1$ ave. in $\times 10^4$	$(\sigma/p)_2$ in $\times 10^4$	$(\sigma/p)_2$ ave. in $\times 10^4$	K_1 ft	K_2 ft
10	7361	18,453	104.4	16.73	16.85	16.73	16.98	11,240	11,320
13	7375		101.5	16.97		17.22			
14	7276		245	18.62	18.19	17.26	17.42	12,130	11,610
15	7505		247	17.76		17.58			
16	7413		476	17.06	17.48	19.87	20.12	11,650	13,310
17	7434		477	17.78		20.38			

Table 3. Impact Test Results on 5052 H-39 Aluminum
Honeycomb Material

Test No.	W_p grams	W_m grams	V_o ft/sec	$(\sigma/p)_1$ in $\times 10^4$	$(\sigma/p)_1$ ave. in $\times 10^4$	$(\sigma/p)_2$ in $\times 10^4$	$(\sigma/p)_2$ ave. in $\times 10^4$	K_1 ft	K_2 ft
29	7490	22,199	467	21.69	23.56	24.54		18,850	19,590
32	7520		452	25.44					

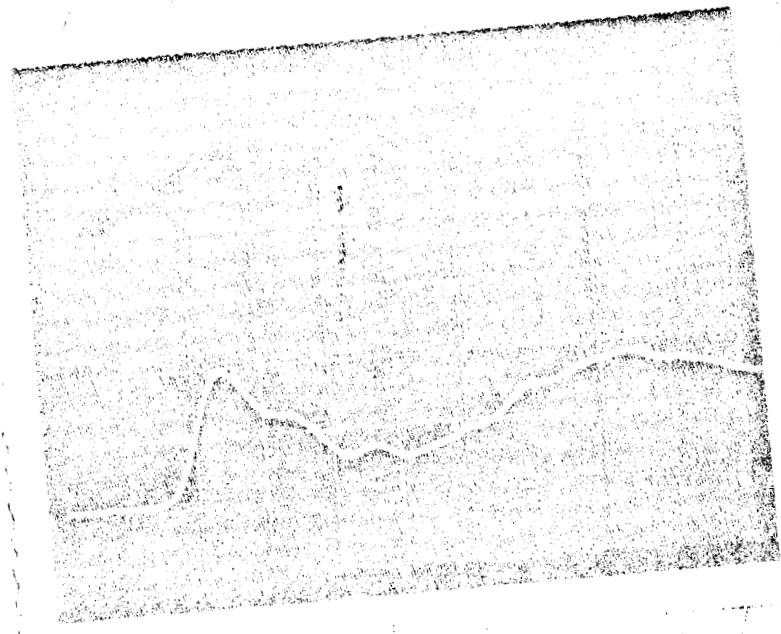
Table 4. Impact Test Results on Balsa Wood-Impacted
Parallel to Grain

Length	Density lb/in ³	V ₀ , Impact Velocity ft/sec	Remarks
8	.005076	164	Specimen crushed from both ends, considerable delamination
0	.005076	169	Same as test no. 1
0	.005076	125	Specimen taped about its base, overall column type buckling produced eccentric crushing
0	.004970	111	Specimen taped about its base; with shorter length specimen crushed uniformly
0	.004975	252	Specimen taped about its base; some delamination
0	.004850	484	Specimen was entirely fragmented
0	.004949	475	Specimen was entirely fragmented
0	.004594	104.4	Specimen crushed uniformly from impacted end, no delamination
0	.004679	101.5	Specimen crushed from both ends; a minor delamination produced eccentric crushing
0	.004789	245	Specimen crushed uniformly from impacted end
0	.004679	247	Specimen crushed uniformly from both ends
0	.004667	476	Same as test no. 15
0	.004719	477	Same as test no. 15
0	.004401	467	Specimen was entirely fragmented
0	.004481	452	Specimen splintered apart and buckled

Table 1.

Test No.	Specimen Material	Cross-Sectional Area - in ²	L, in
1	Nylon-Phenolic Fiberglass Honey- comb, 3/16 in. cell size	12.75	7.
2		12.25	8.
3		12.25	8.
4		12.25	6.
6		12.14	6.
7		12.25	6.
18	✓	12.25	6.
10	5052 H-39 Aluminum Honeycomb, 3/16 in cell size, .003 in foil thickness	12.25	6.
13		12.25	6.
14		12.25	6.
15		12.25	6.
16		12.25	6.
17		12.25	6.
19	Balsa Wood	16.00	2.
22	Balsa Wood	16.00	5.

Deceleration (190.9 g/div.) →



Time (100 μ sec./div.) →

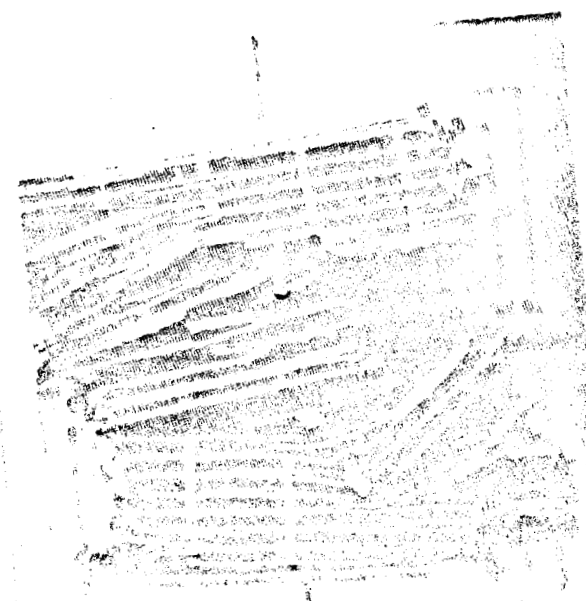
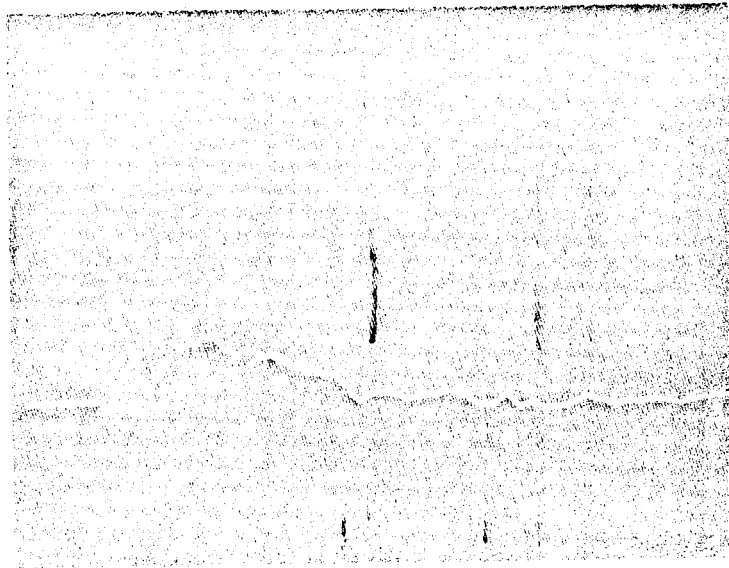


Fig. 1 ACCELEROMETER RECORD AND SPECIMEN AFTER IMPACT
(TEST NO. 1) - NYLON-PHENOLIC FIBERGLASS HONEYCOMB
AT 1000 PSI - IMPACT FROM LEFT

Deceleration (190.9 g/div.) →



Time (.001 sec./div.) →

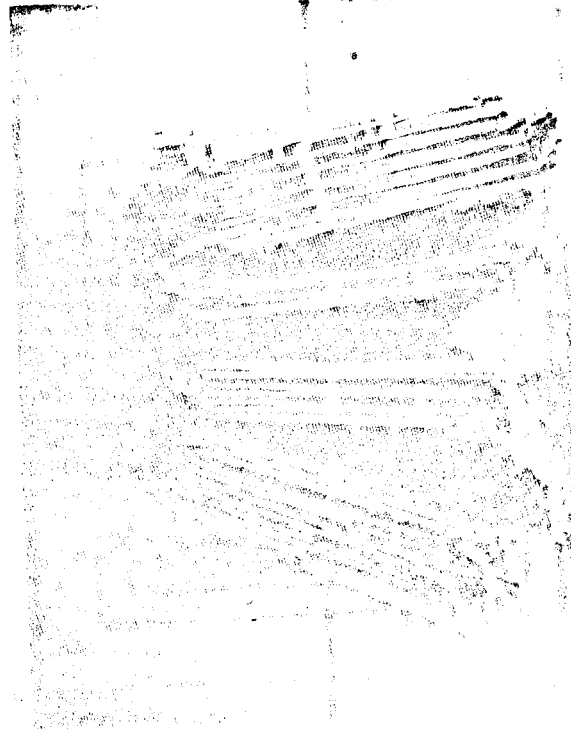
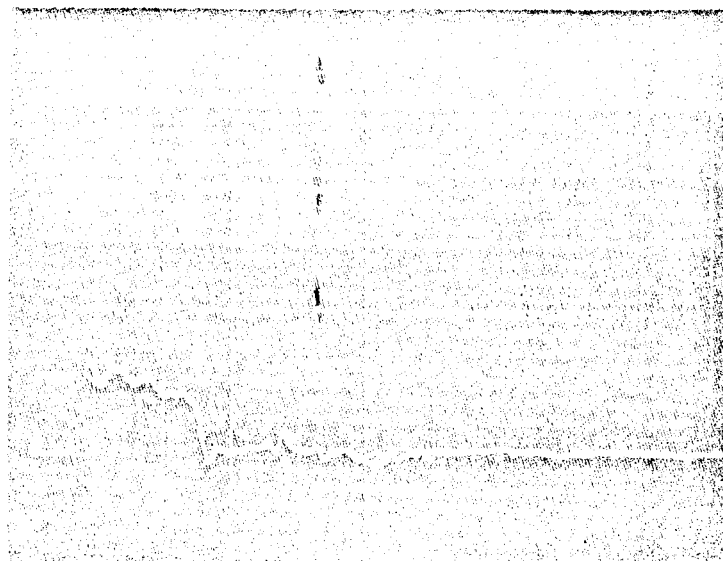


Fig. 2 ACCELEROMETER RECORD AND SPECIMEN AFTER IMPACT
(TEST NO. 2) - NYLON-EPHOLIC FIBERGLAST HONEYCOMB
AT V = 1400 ft./sec. IMPACT FROM LEFT

Acceleration (190.9 g/div.) →



Time (.001 sec./div.) →

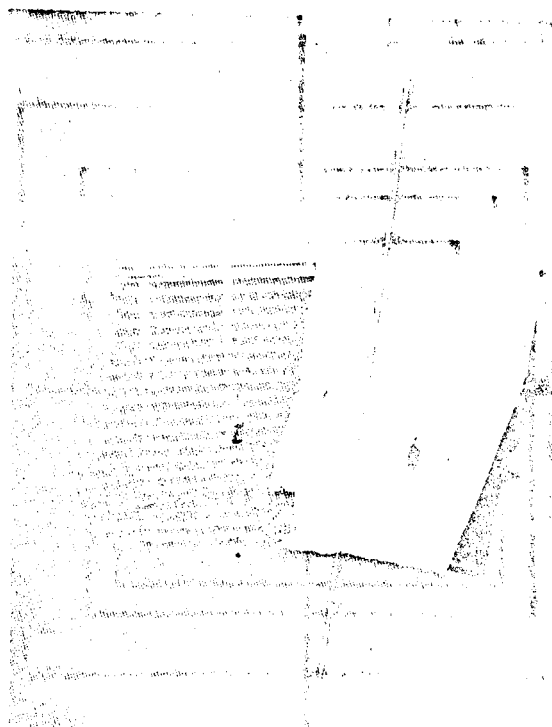
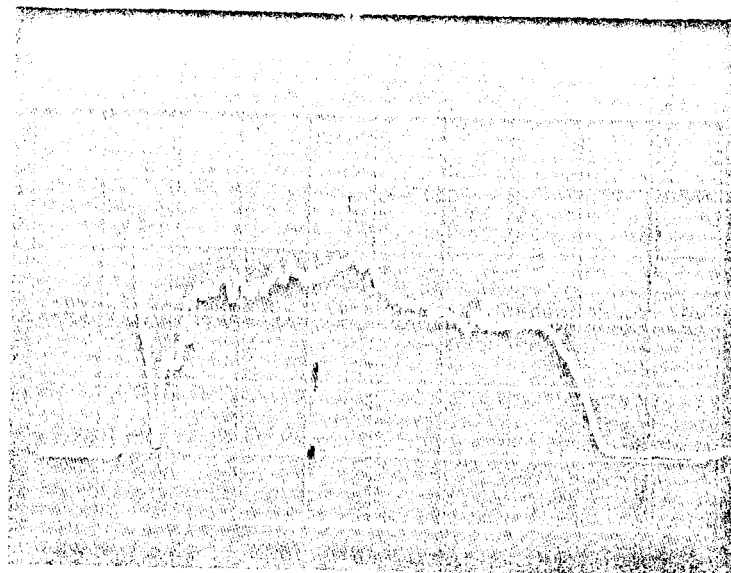


Fig. 3 ACCELEROMETER RECORD AND SPECIMEN AFTER IMPACT
(TEST NO. 3) - NYLON-PHENOLIC FIBERGLASS HONEYCOMB
IMPACT - 100 G. - IMPACT FROM LEFT

Deceleration (95.5 g/div.) →



Time (500 μ sec./div.) →

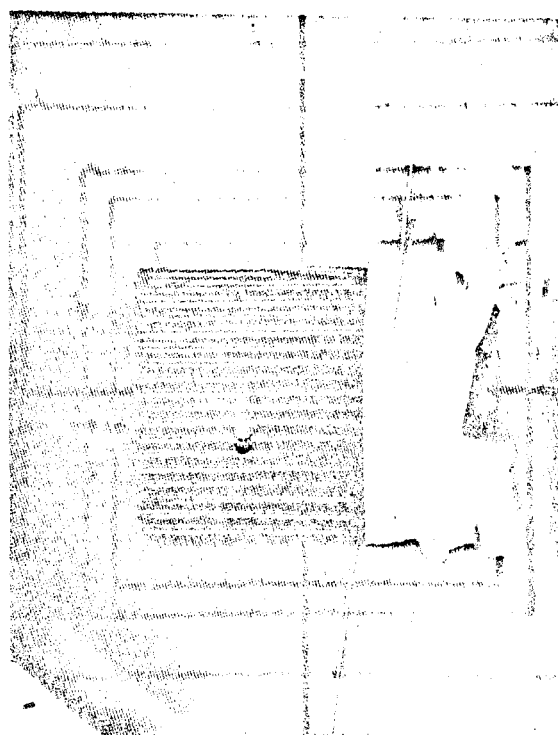
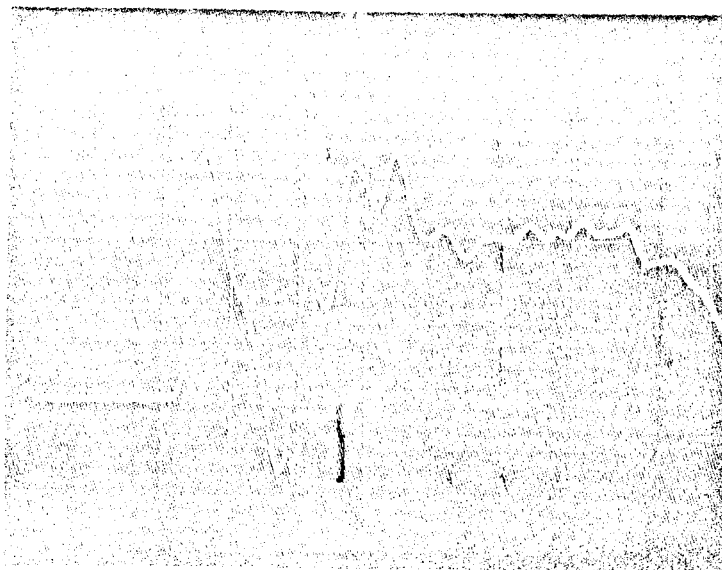


Fig. 4 ACCELEROMETER RECORD AND SPECIMEN AFTER IMPACT
(TEST NO. 4) - NYLON-PHENOLIC FIBERGLASS HONEYCOMB
AT $V_0 = 111$ ft./sec. - IMPACT FROM LEFT

Deceleration (95.5 g/div.) →



Time (300 μ sec./div.) →

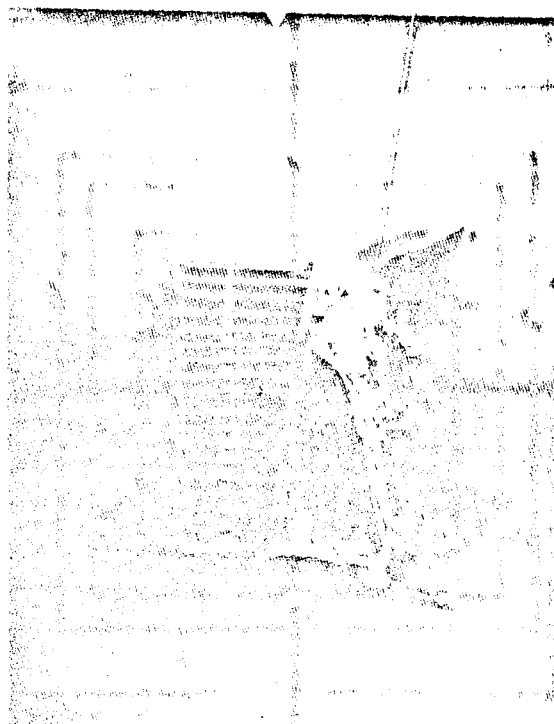
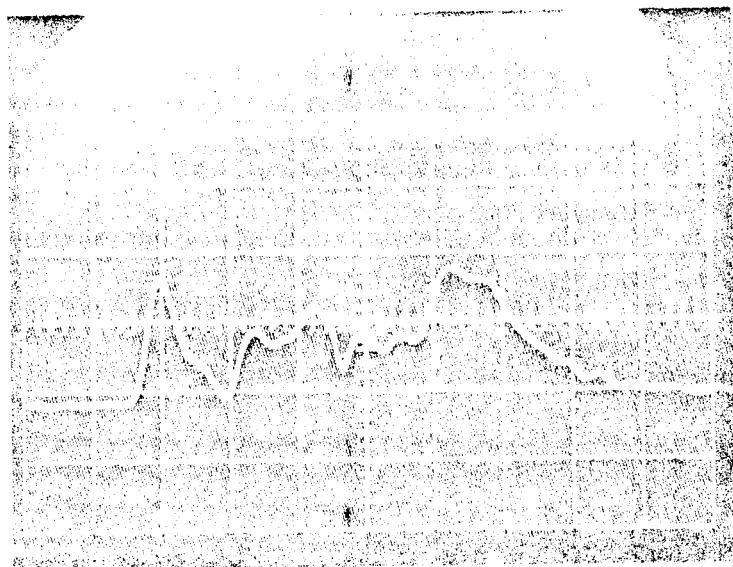


Fig. 5 ACCELEROMETER RECORD AND SPECIMEN AFTER IMPACT
(TEST NO. 6) - NYLON-PHENOLIC FIBERGLASS HONEYCOMB
AT $V_0 = 257$ ft./sec. - IMPACT FROM LEFT

Deceleration (190.9 g/cm) →

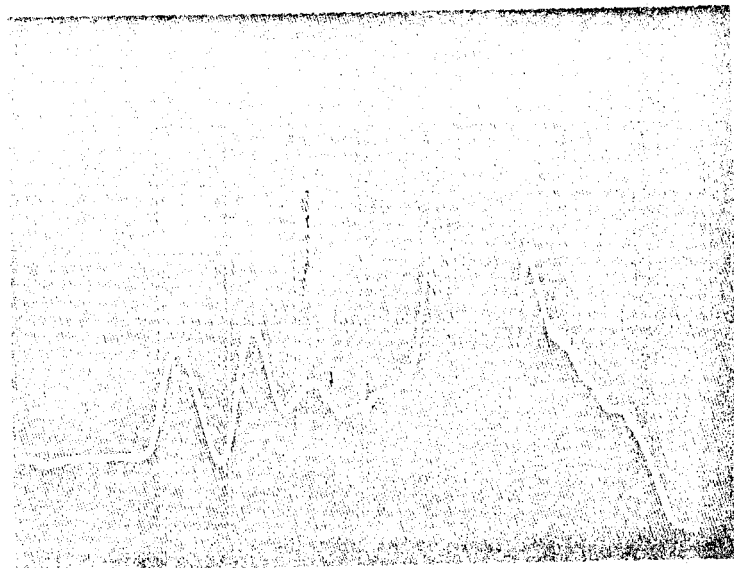


Time (200 μ sec./div.) →

(Specimen was entirely fragmented.)

Fig. 6 ACCELEROMETER RECORD AND SPECIMEN AFTER IMPACT
(TEST NO. 7) - NYLON-PHENOLIC FIBERGLASS HONEYCOMB
AT $V_0 = 484$ ft./sec. - IMPACT FROM LEFT

Deceleration (100.9 g/div.) \rightarrow

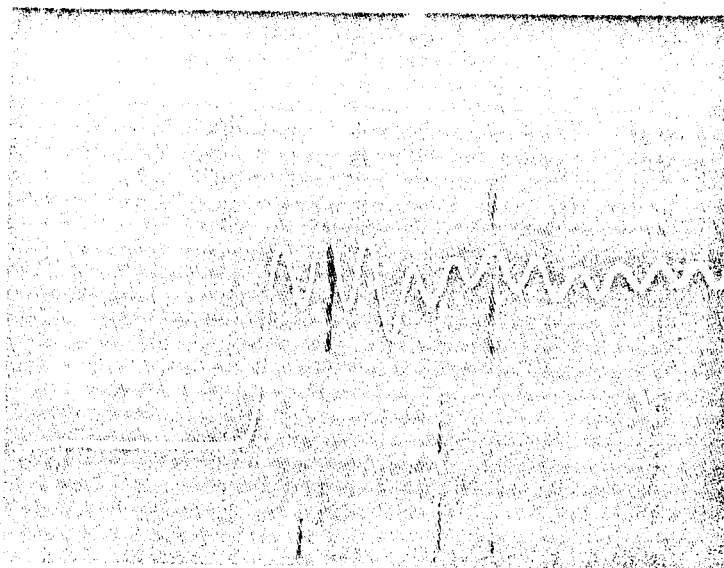


Time (200 μ sec./div.) \rightarrow

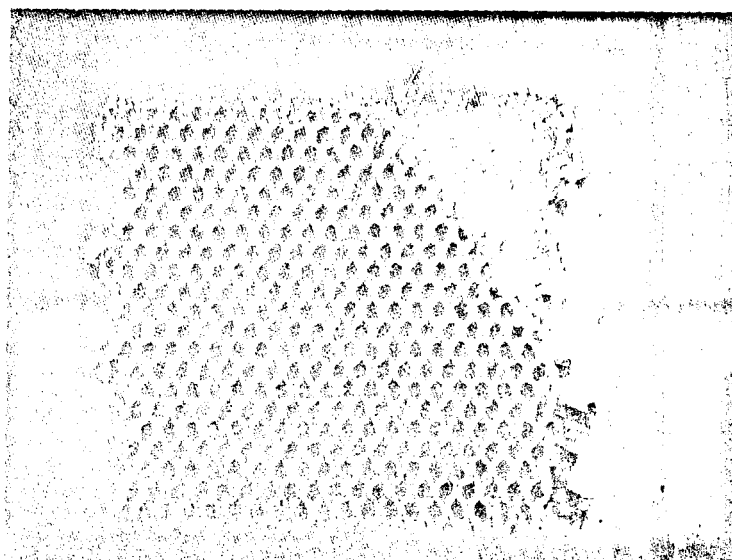
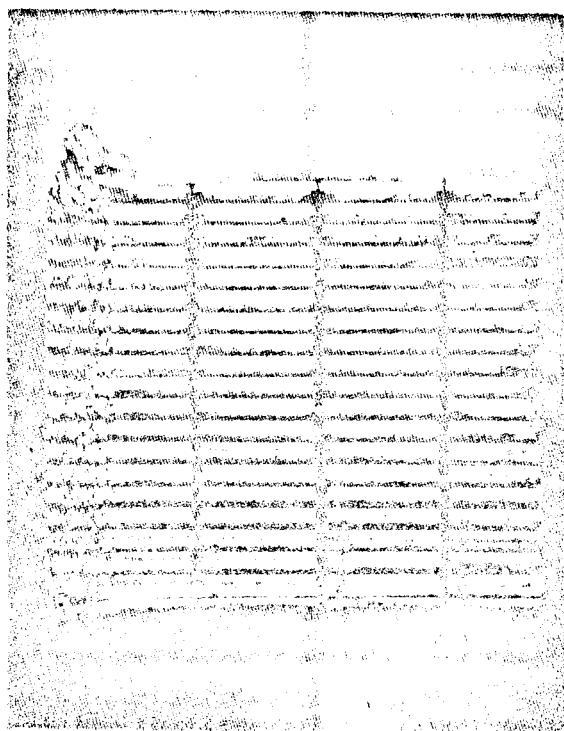
(Specimen was entirely fragmented.)

Fig. 7 ACCELEROMETER RECORD AND SPECIMEN AFTER IMPACT
(TEST NO. 19) - NYLON-PHENOLIC FIBERGLASS HONEYCOMB
AT $V_0 = 475$ ft./sec. - IMPACT FROM LEFT

Deceleration (95.5 g/div.) →



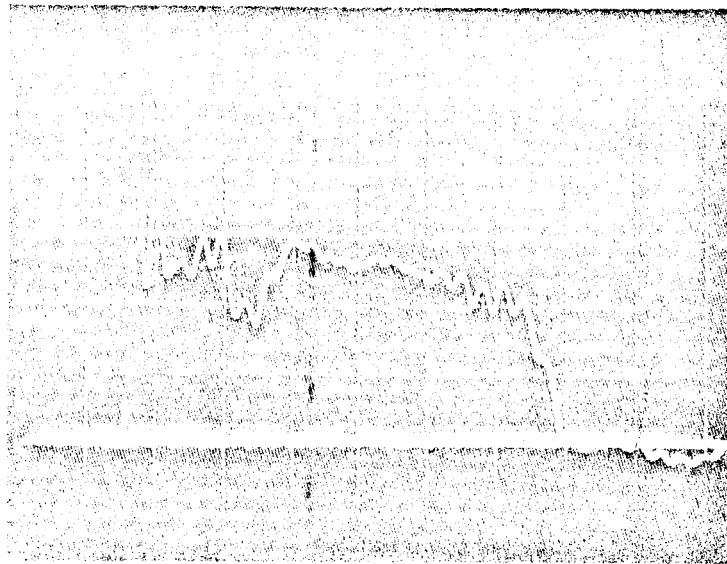
Time (200 μ sec./div.) →



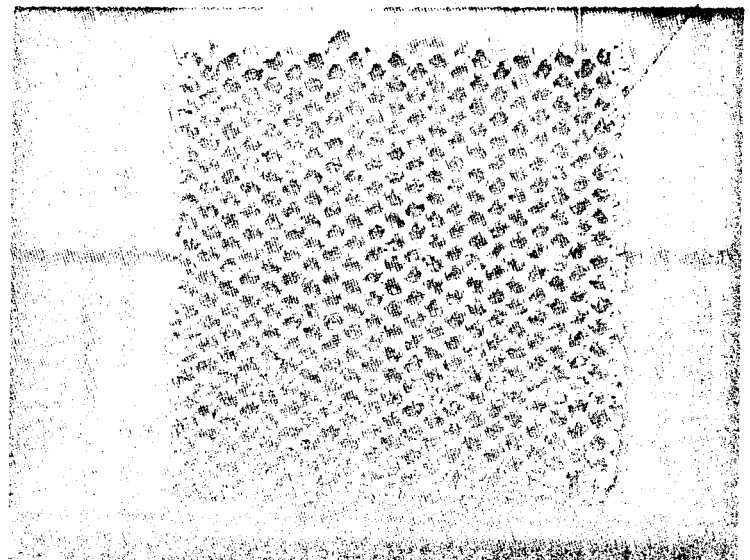
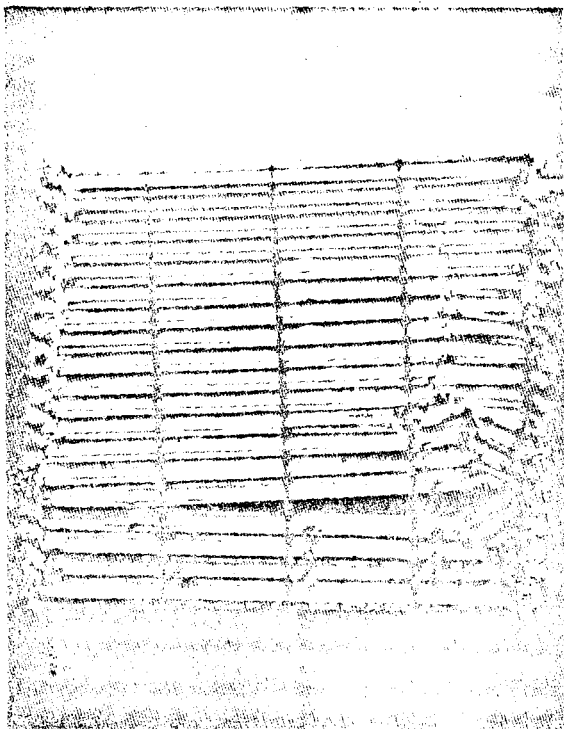
(Front View of Impacted End)

Fig. 8 ACCELEROMETER RECORD AND SPECIMEN AFTER IMPACT
(TEST NO. 10) - 5052 H-19 ALUMINUM HONEYCOMB
AT $V_0 = 104.4$ ft./sec. - IMPACT FROM LEFT

Deceleration (95.5 g/div.) →



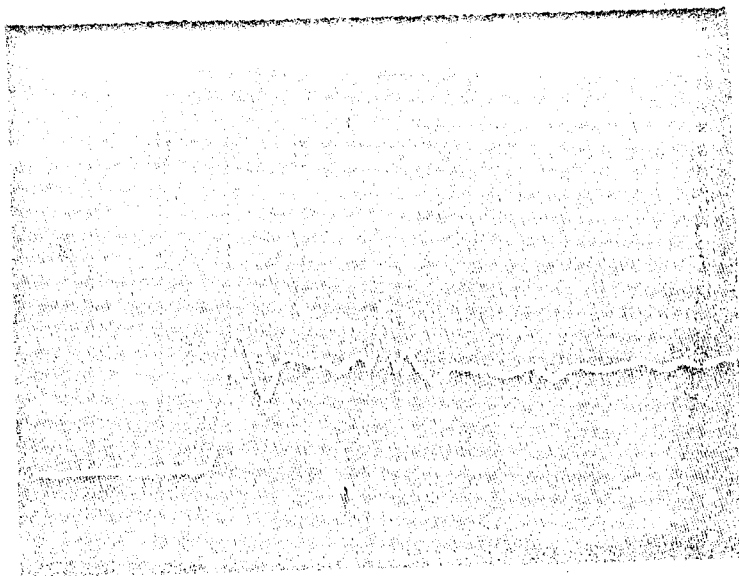
Time (500 μ sec./div.) →



(Front View of Impacted End)

Fig. 9 ACCELEROMETER RECORD AND SPECIMEN AFTER IMPACT
 (TEST NO. 13) - 5052 H-39 ALUMINUM HONEYCOMB
 AT $V_0 = 101.5$ G./sec. - IMPACT FROM LEFT

Acceleration (190.9 g/div.) →



Time (200 μ sec./div.) →

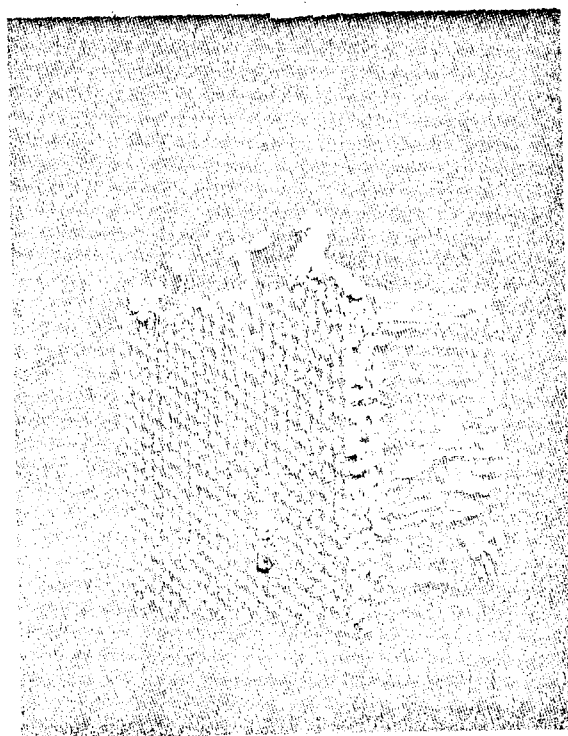
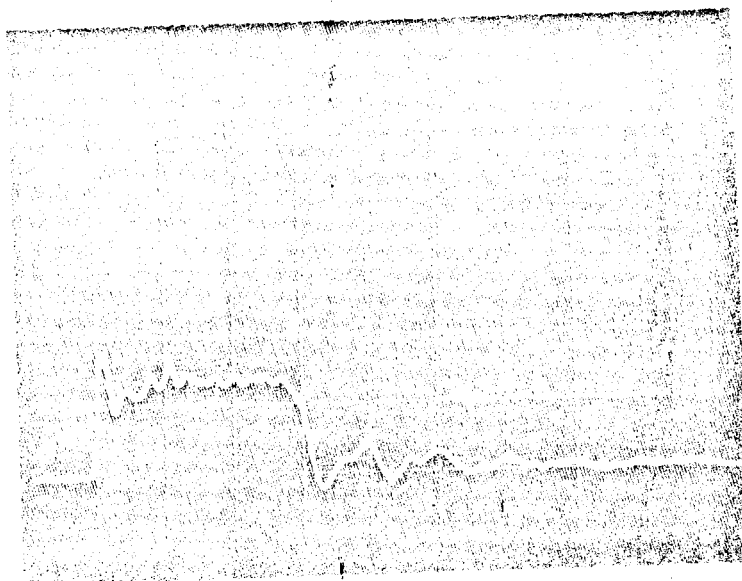


Fig. 10 ACCELEROMETER RECORD AND SPECIMEN AFTER IMPACT
(TEST NO. 14) - 5052-B-35 ALUMINUM HONEYCOMB
AT $V_i = 215$ ft./sec. - IMPACT FROM LEFT

Deceleration (190.9 g/cm) →



Time (500 μ sec./div.) →

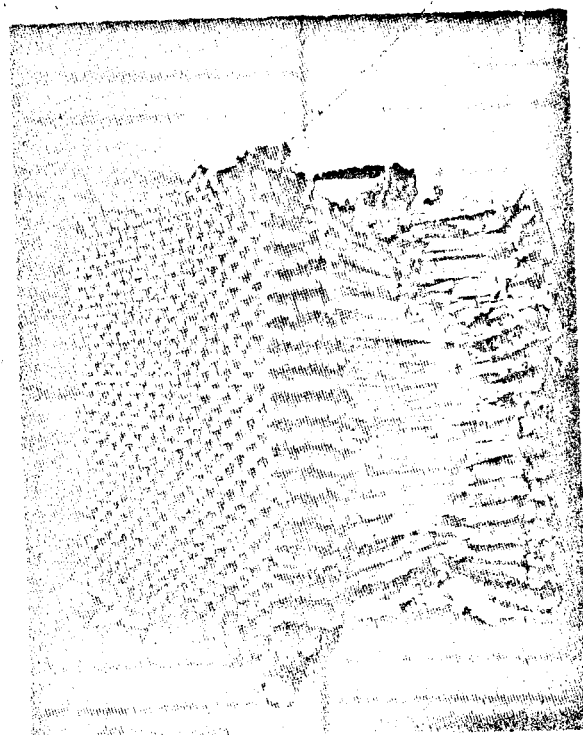
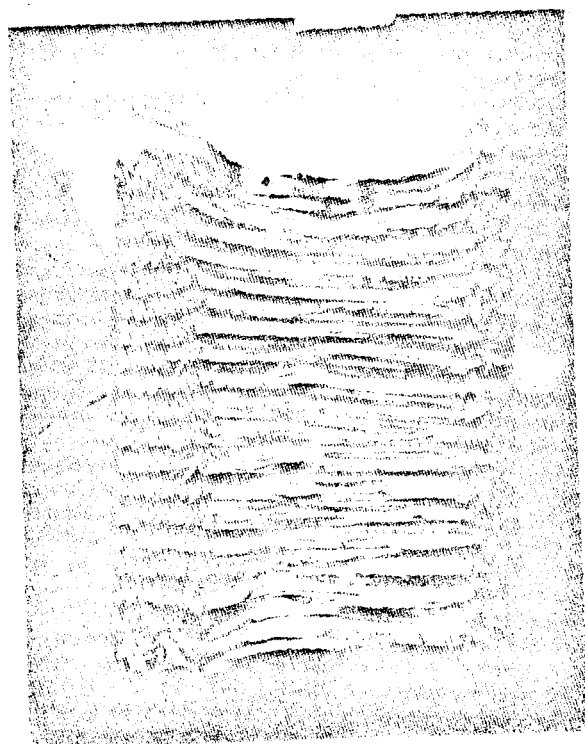
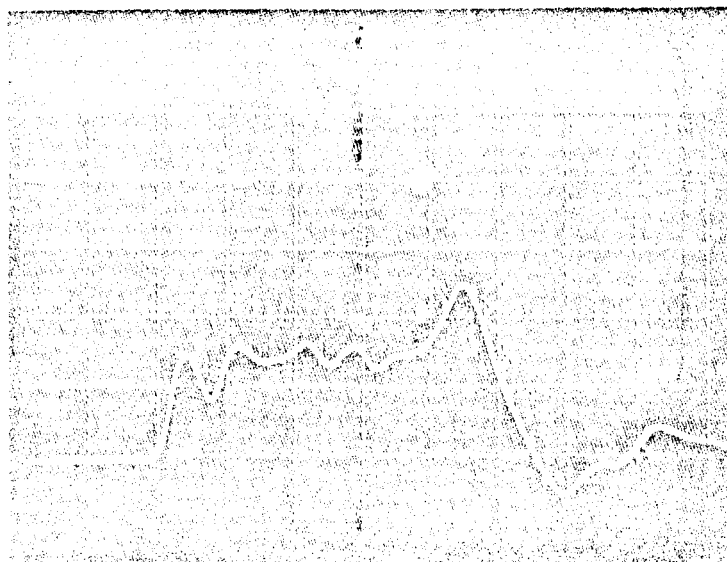
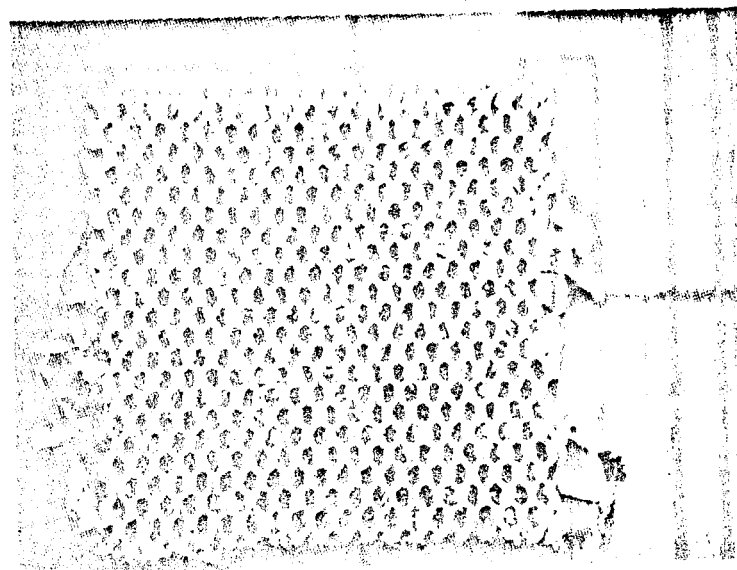
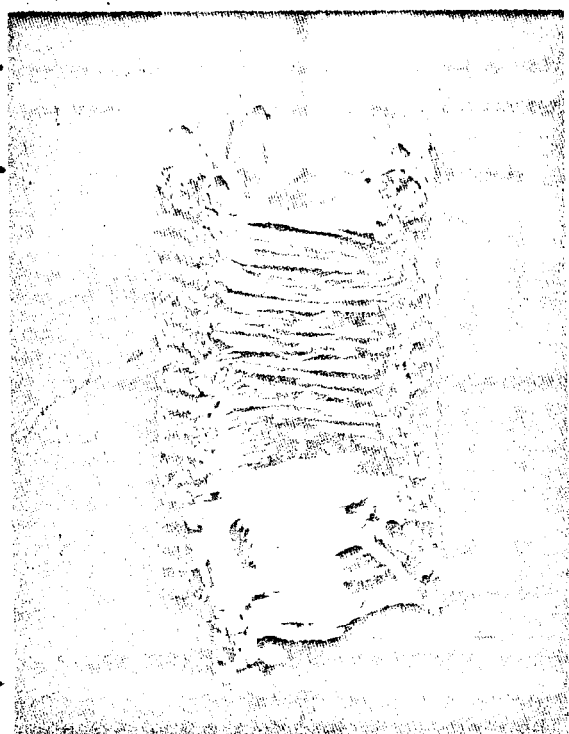


Fig. 11 ACCELEROMETER RECORD AND SPECIMEN AFTER IMPACT
(TEST NO. 15) - 5052 H-39 ALUMINUM HONEYCOMB
AT $V_0 = 747$ ft./sec. - IMPACT FROM LEFT

Deceleration (190.9 g/div.) →



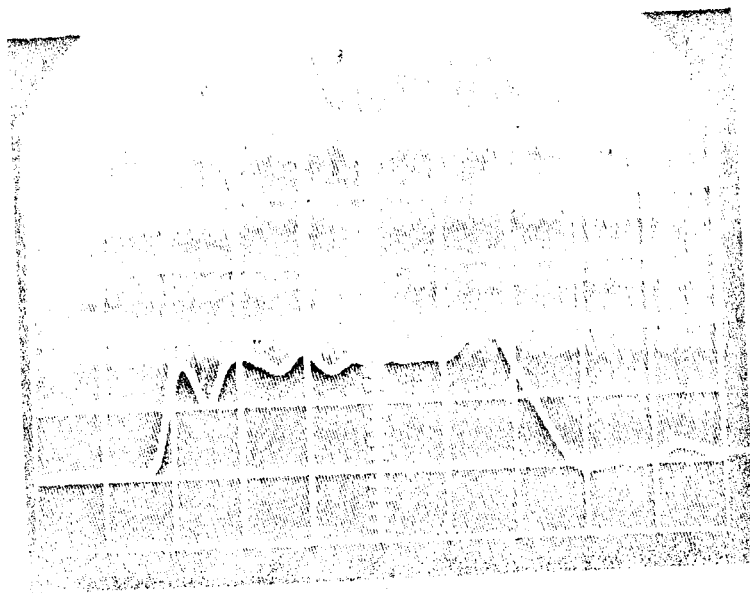
Time (200 μ sec./div.) →



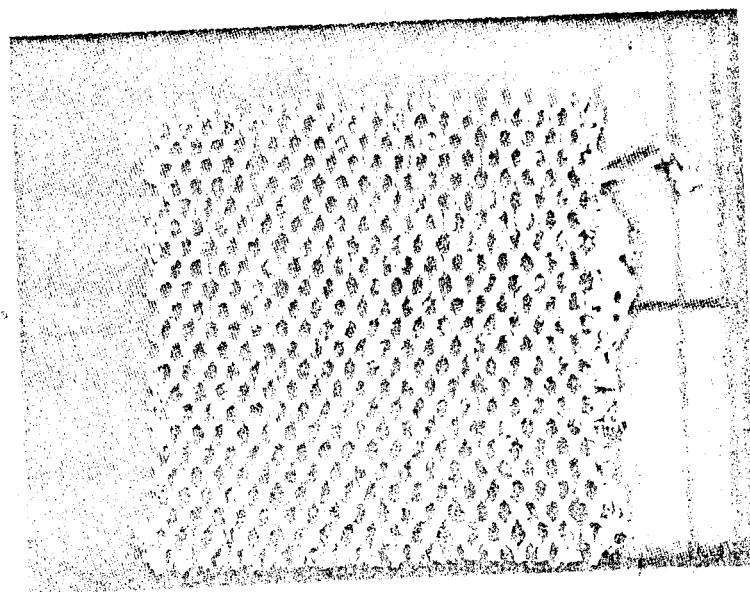
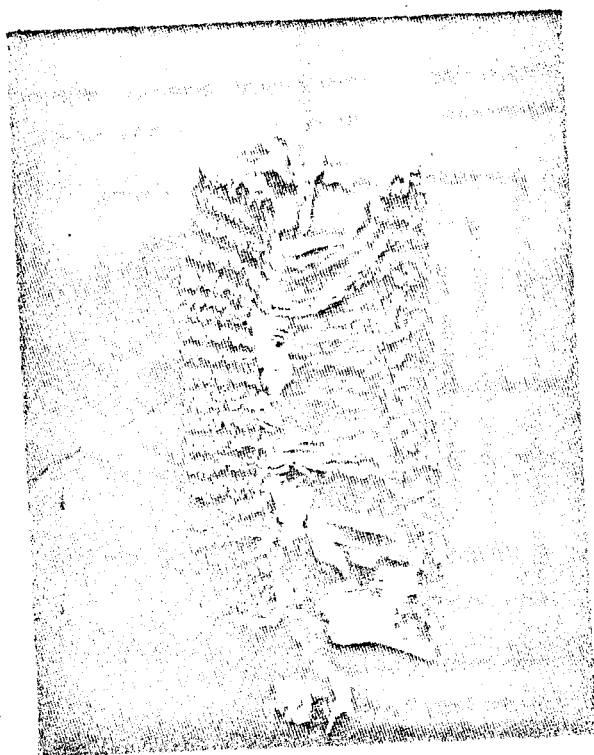
(Front View of Impacted End)

Fig. 12 ACCELEROMETER RECORD AND SPECIMEN AFTER IMPACT
(TEST NO. 16) - 5932-H-69 ALUMINUM HONEYCOMB
AT $V_0 = 475$ ft./sec. - IMPACT FROM LEFT

Deceleration (190.9 g/div.) →



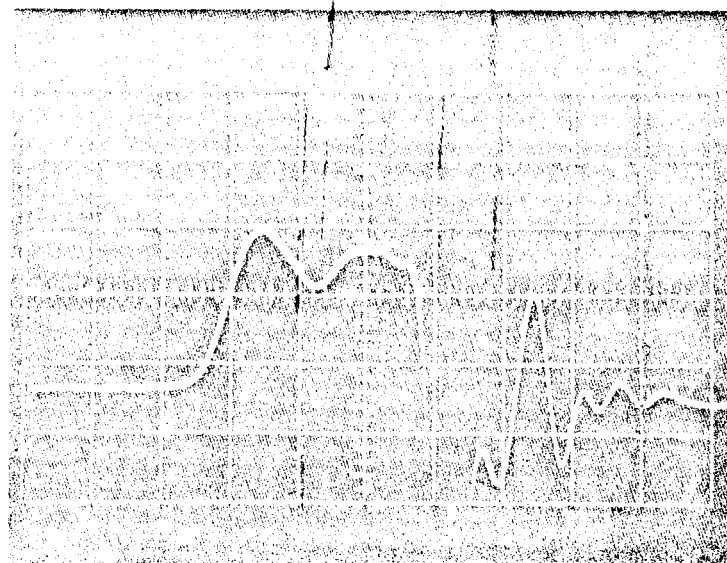
Time (200 μ sec./div.) →



(Front View of Impacted End)

Fig. 13 ACCELEROMETER RECORD AND SPECIMEN AFTER IMPACT
(TEST NO. 17) - 5052 H-39 ALUMINUM HONEYCOMB
AT $V_0 = 477$ ft./sec. - IMPACT FROM LEFT

Deceleration (190.9 g/div.) →



Time (100 μ sec./div.) →

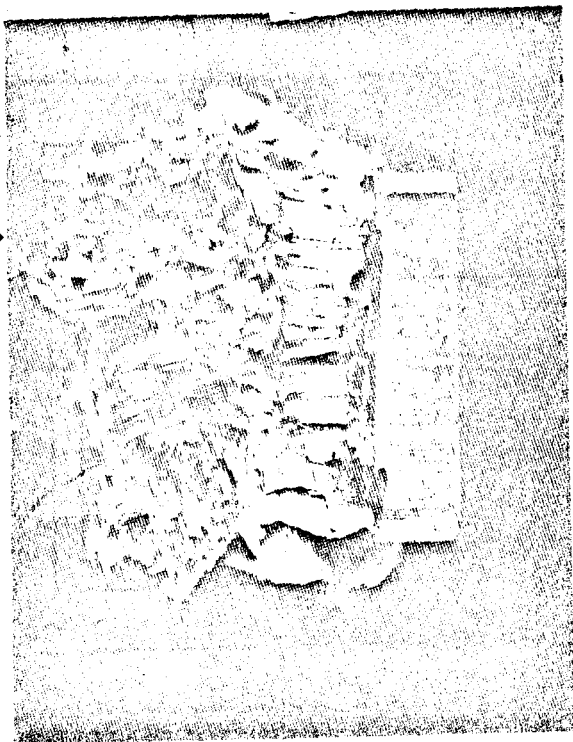
(Specimen was entirely fragmented.)

Fig. 14 ACCELEROMETER RECORD AND SPECIMEN AFTER IMPACT
(TEST NO. 19) - BALSA WOOD AT $V_0 = 467$ ft./sec.
IMPACT FROM LEFT

Deceleration (223 g/div.) →



Time (100 μ sec./div.) →



(Front View of Impacted End)

Fig. 15 ACCELEROMETER RECORD AND SPECIMEN AFTER IMPACT
(TEST NO. 22) - BALSA WOOD AT $V_0 = 452$ ft./sec.
IMPACT FROM LEFT

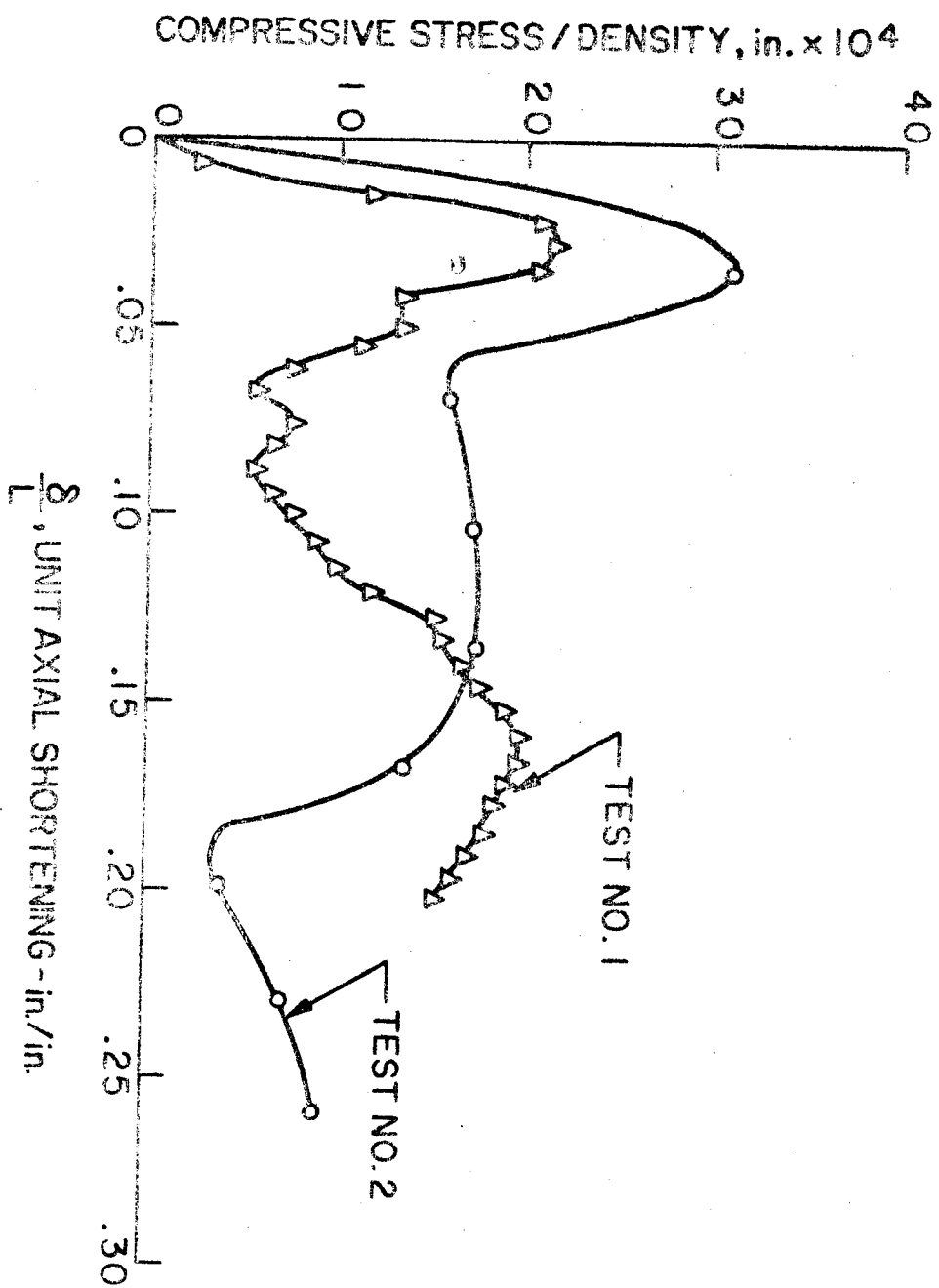


Fig. 16 STRESS-DENSITY RATIO VS. STRAIN FOR NYLON-PHENOLIC FIBERGLASS HONEYCOMB UNDER AXIAL IMPACT LOADING.

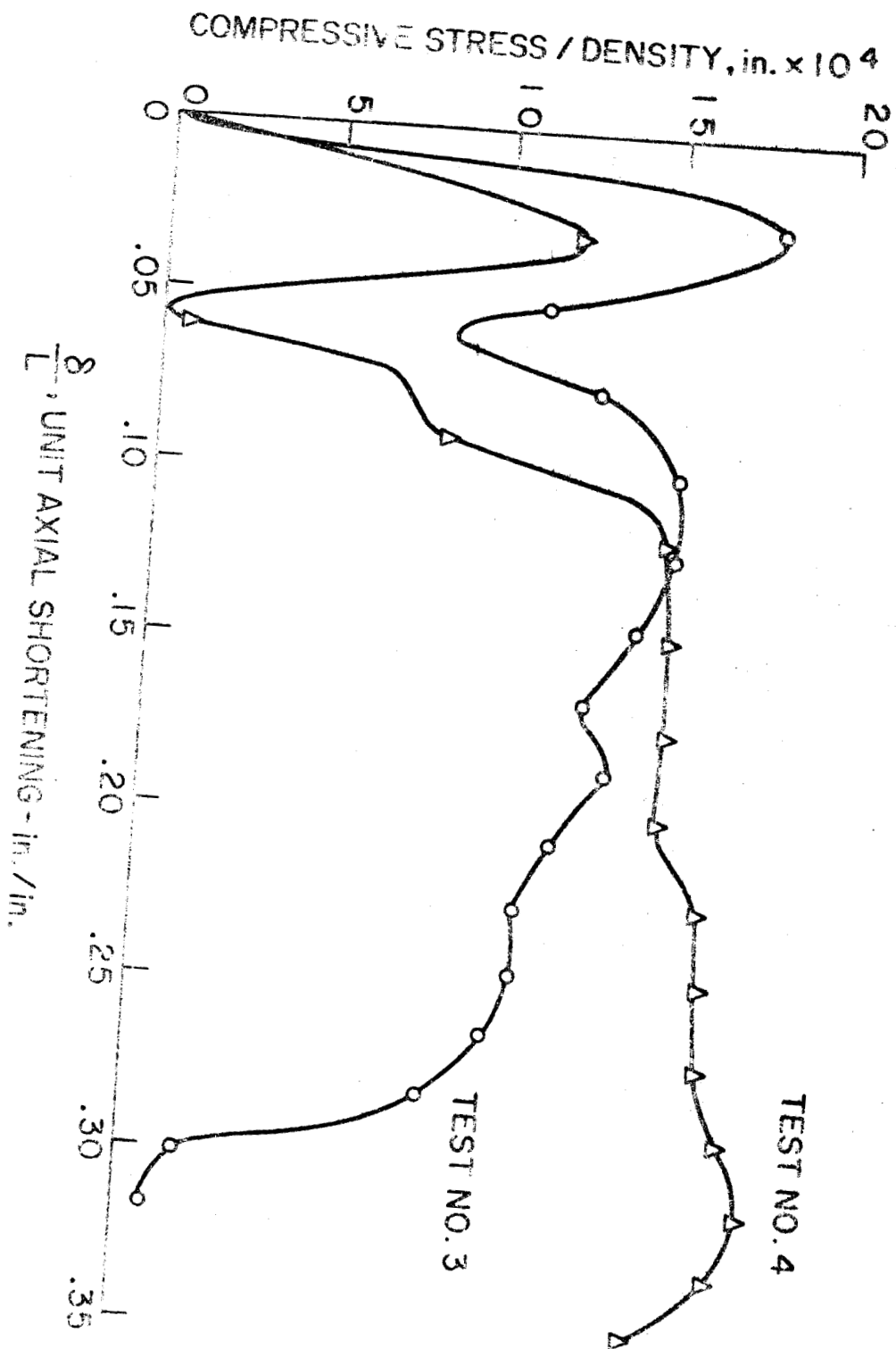


Fig. 17
STRESS-DENSITY RATIO VS. STRAIN FOR NYLON-PHENOLIC
-FIBERGLASS HONEYCOMB UNDER AXIAL IMPACT LOADING.

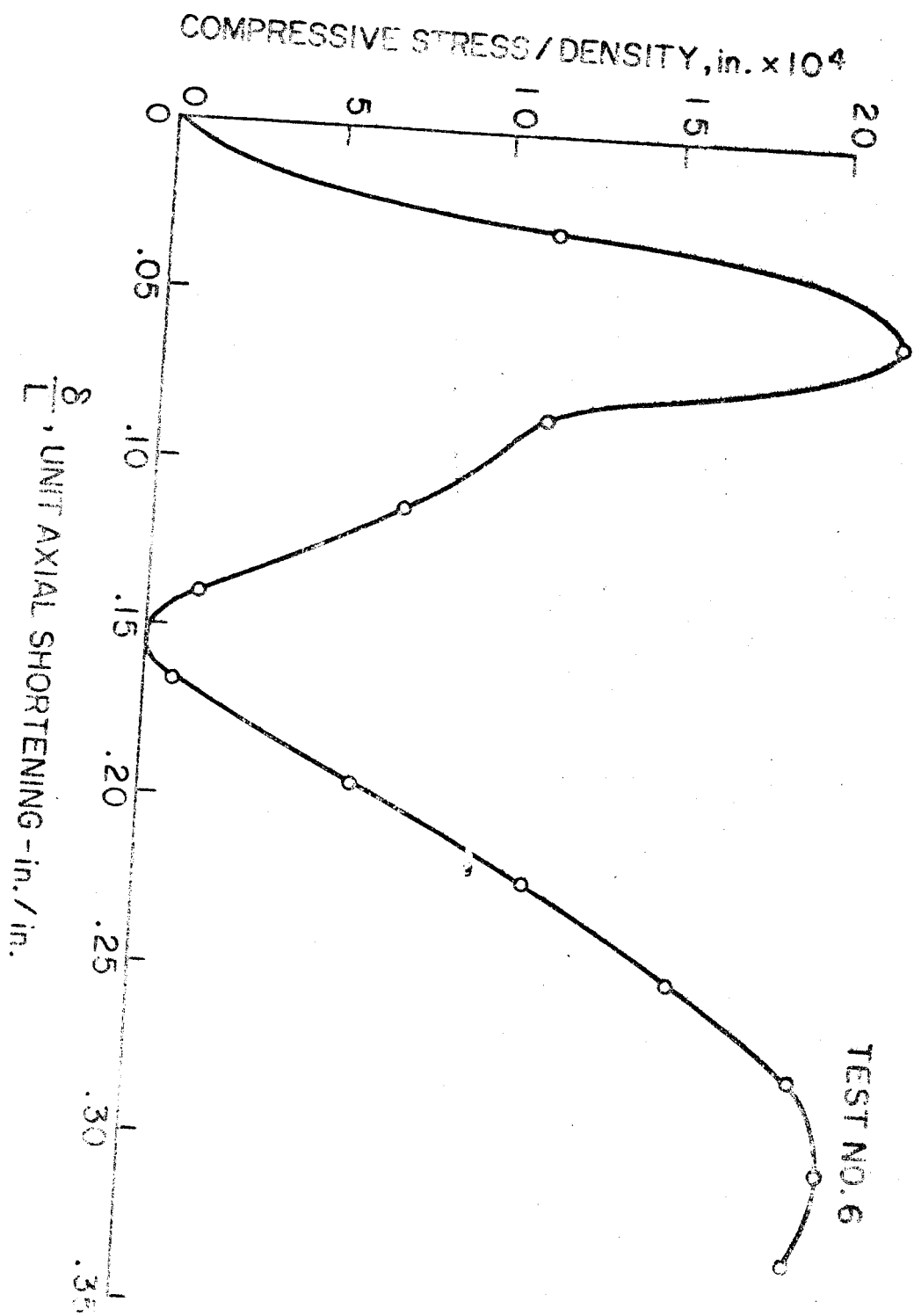


Fig. 18 STRESS-DENSITY RATIO VS. STRAIN FOR NYLON-PHENOLIC FIBERGLASS HONEYCOMB UNDER AXIAL IMPACT LOADING.

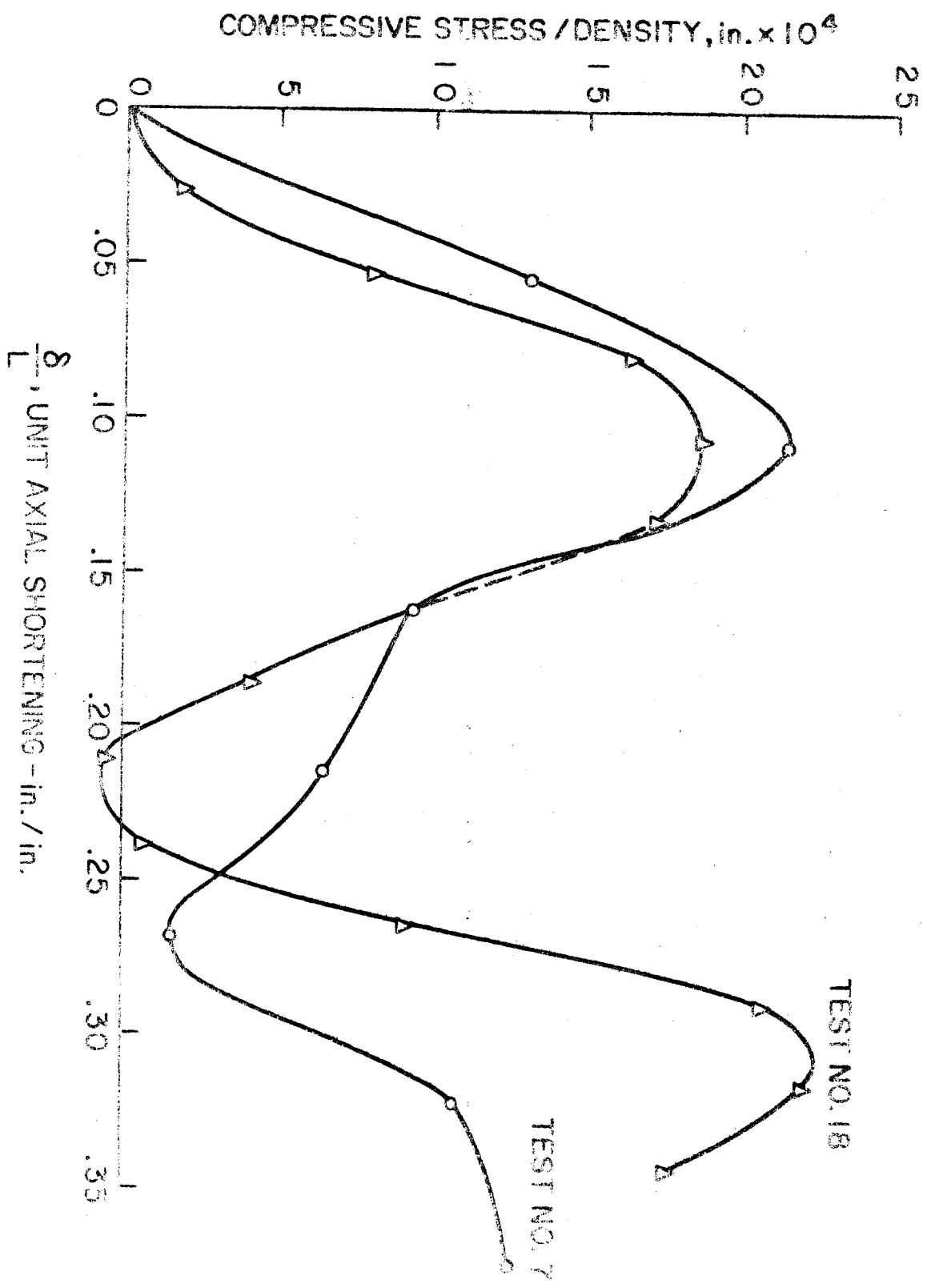


Fig. 19 STRESS-DENSITY RATIO VS. STRAIN FOR NYLON-PHENOLIC FIBERGLASS HONEYCOMB UNDER AXIAL IMPACT LOADING.

○ TEST NO. 10
△ TEST NO. 13

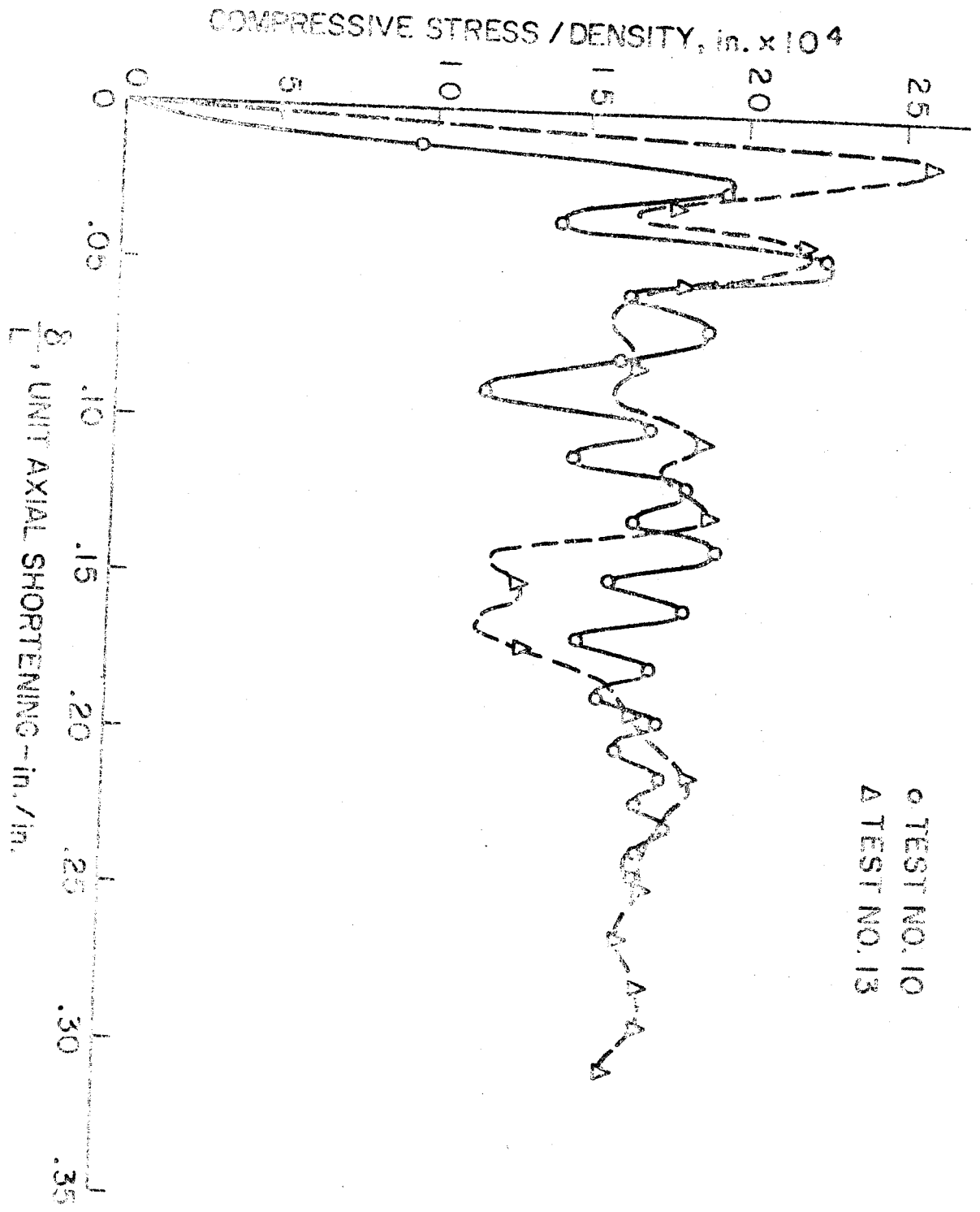


Fig. 20 STRESS-DENSITY RATIO VS. STRAIN FOR 5052 H-39 ALUMINUM
HONEYCOMB UNDER AXIAL IMPACT LOADING.

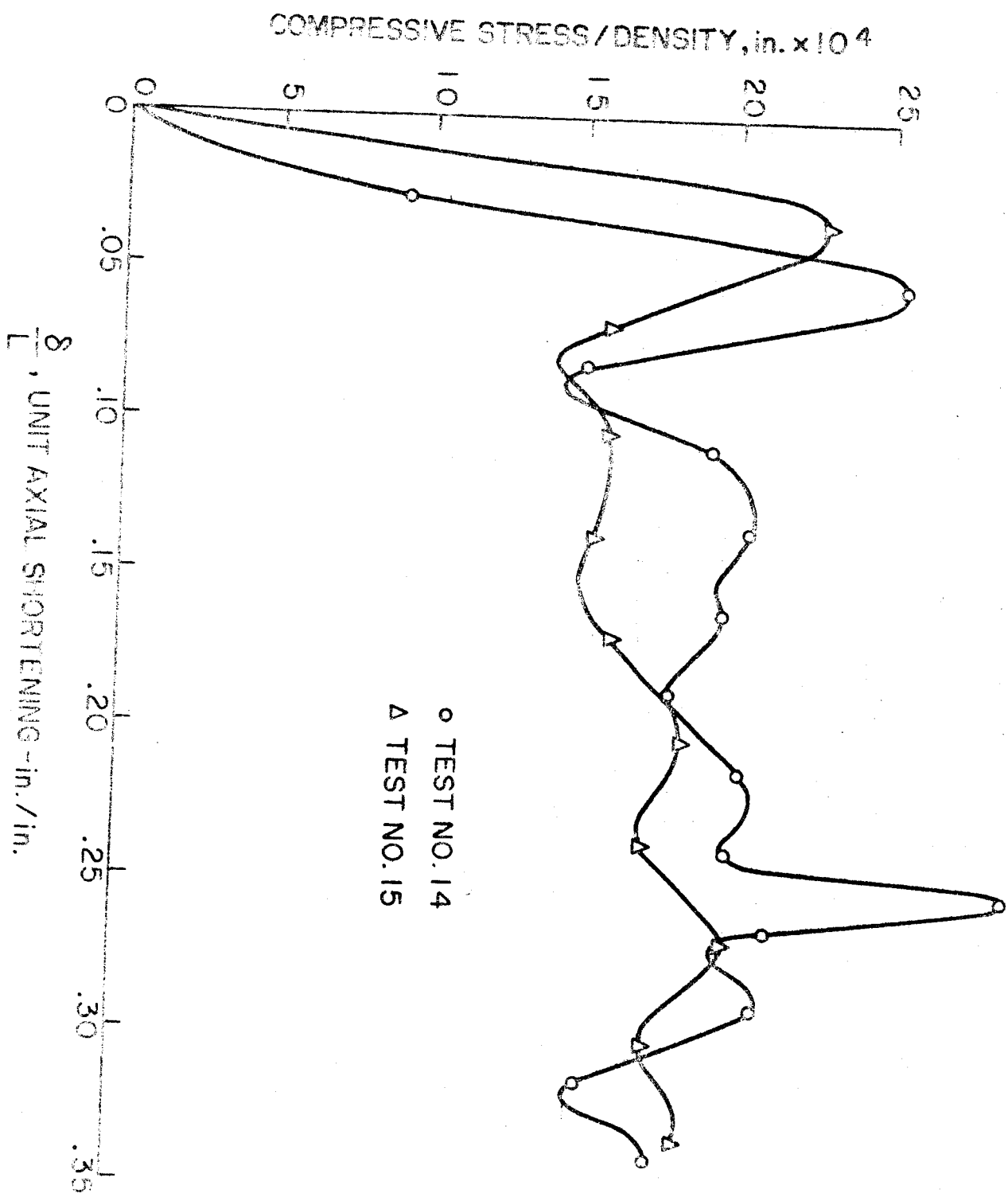


Fig. 21 STRESS-DENSITY RATIO VS. STRAIN FOR 5052 H-39 ALUMINUM
 HONEYCOMB UNDER AXIAL IMPACT LOADING.

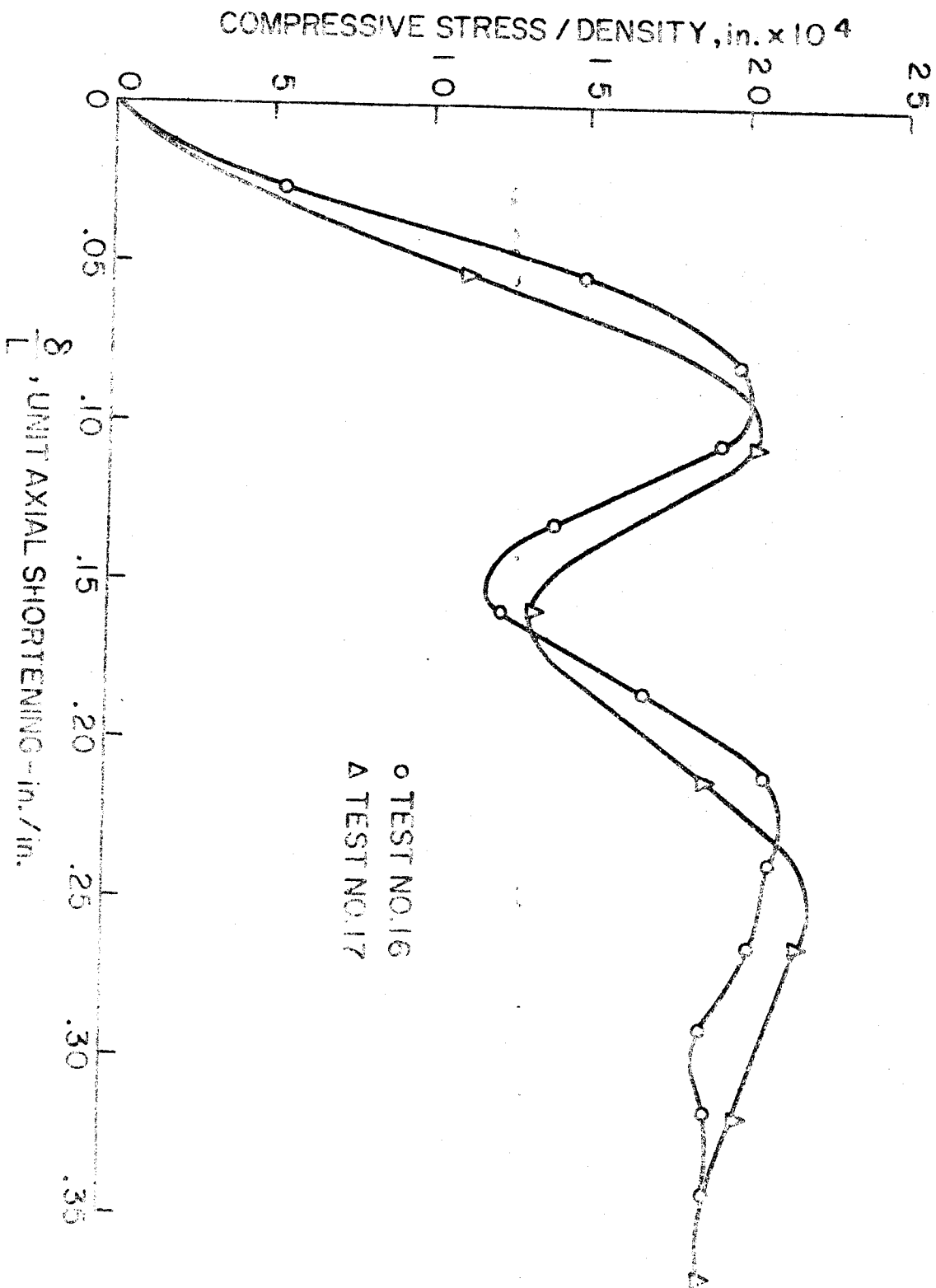
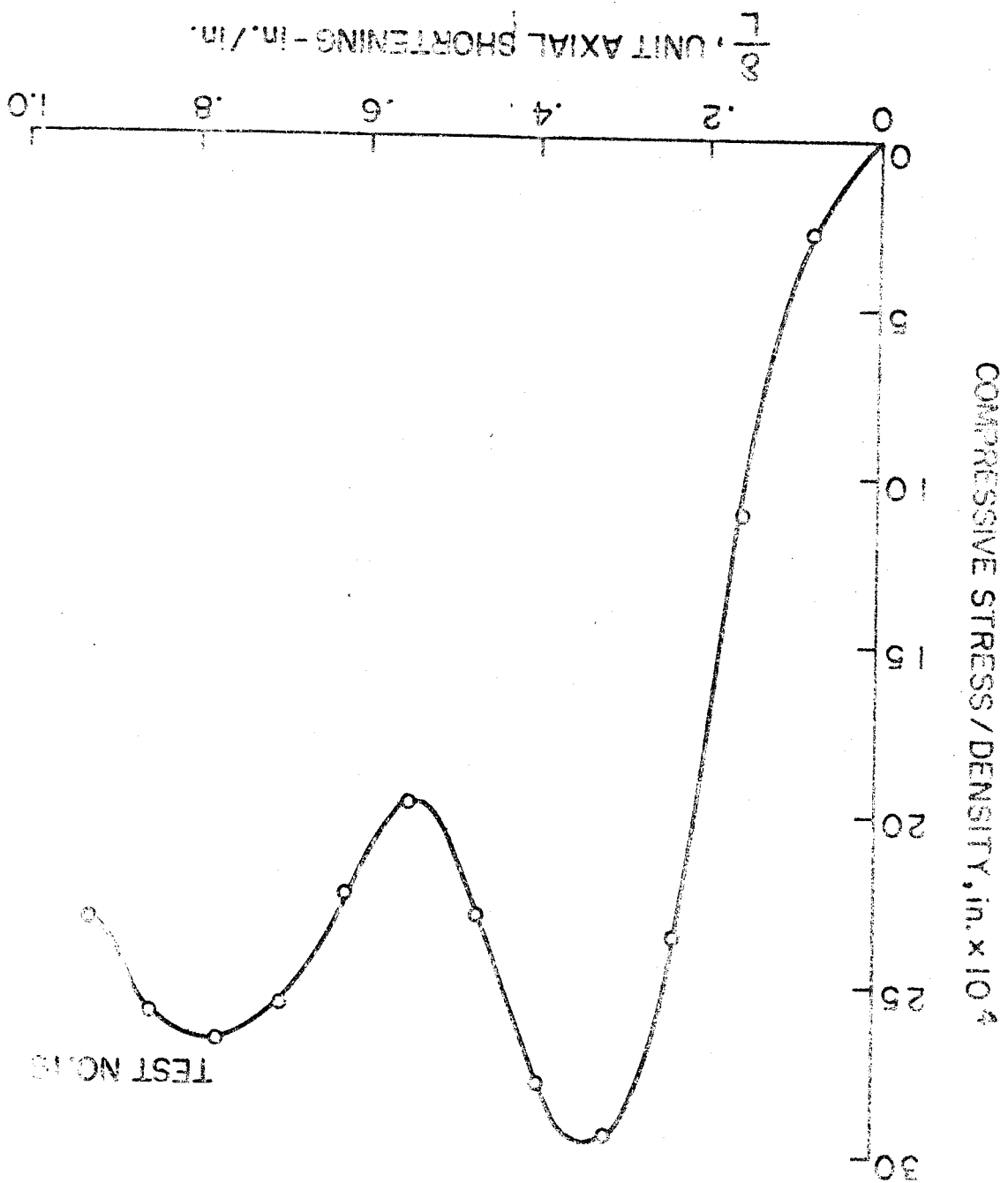


Fig. 22 STRESS-DENSITY RATIO VS. STRAIN FOR 5052 H-39 ALUMINUM
HONEYCOMB UNDER AXIAL IMPACT LOADING.

Fig. 23 STRESS-DENSITY RATIO VS. STRAIN FOR BALSA WOOD
UNDER AXIAL IMPACT LOADING.



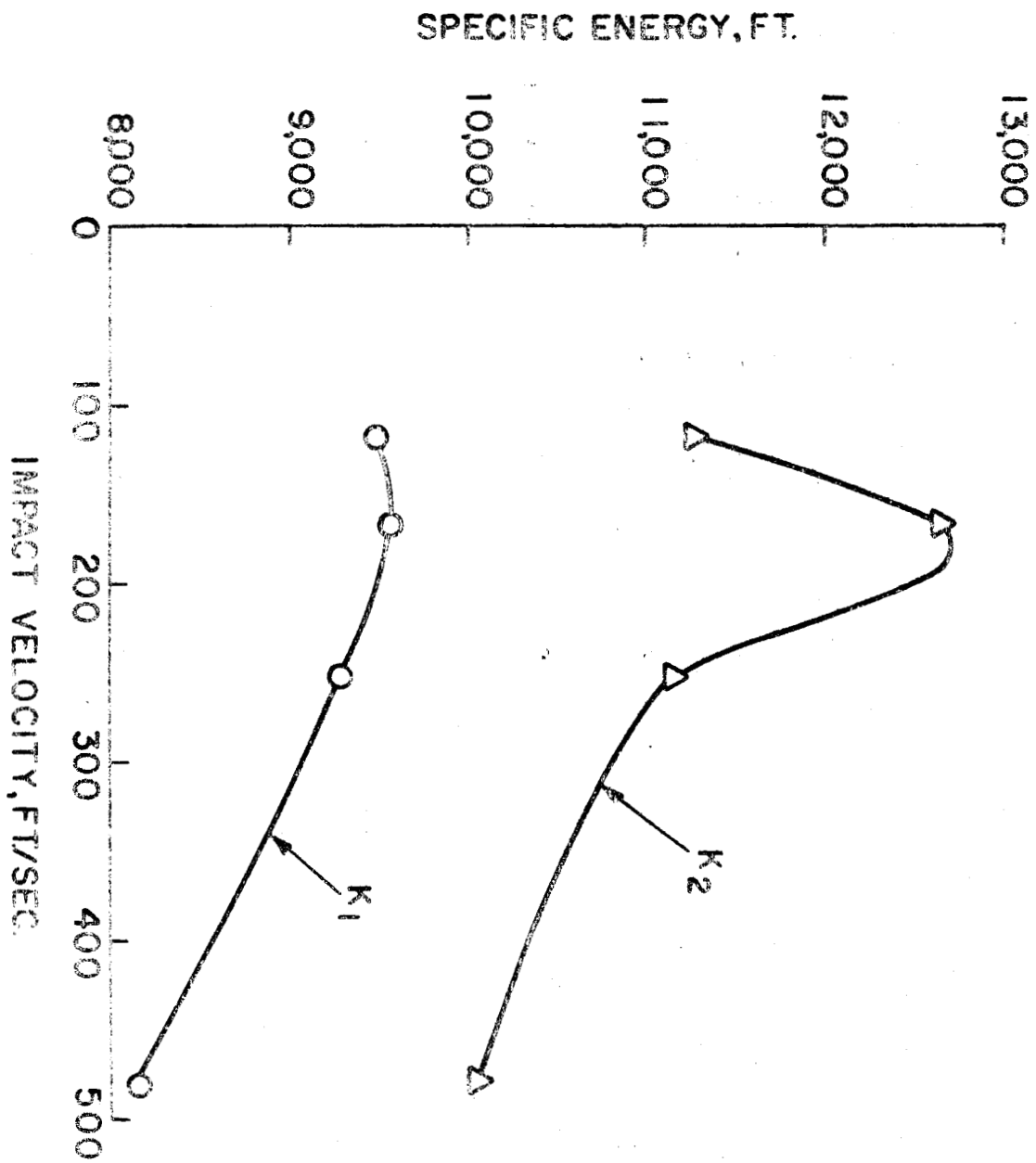


Fig. 24 EFFECT OF IMPACT VELOCITY ON THE SPECIFIC ENERGY OF NYLON-PHENOLIC FIBERGLASS HONEYCOMB.

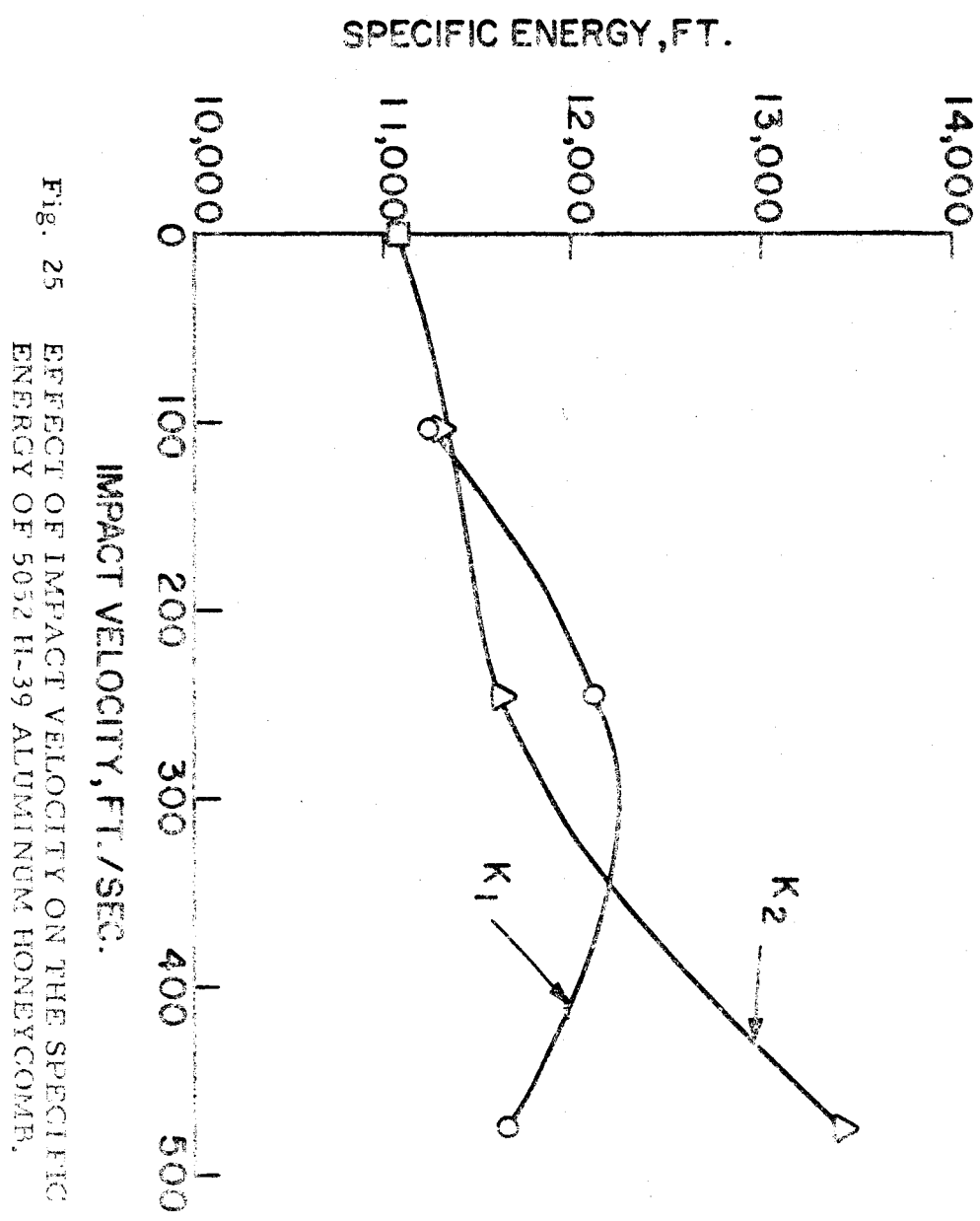


Fig. 25 EFFECT OF IMPACT VELOCITY ON THE SPECIFIC ENERGY OF 5052 H-39 ALUMINUM HONEYCOMB.